Available online at www.sciencedirect.com
ScienceDirect
Journal of Molecular Catalysis A: Chemical 278 (2007) 64–71
JOURNAL OF MOLECULAR CATALYSIS A: CHEMICAL
www.elsevier.com/locate/molcata

BETA zeolite supported on silicon carbide for Friedel-Crafts fixed-bed reactions

Gauthier Winé [a,*], Zora El Berrichi [b], Cuong Pham-Huu [a]

[a] *Laboratoire des Matériaux, Surfaces et Procédés pour la Catalyse (LMSPC)[1], UMR 7515 du CNRS, ECPM, Université Louis Pasteur, 25, rue Becquerel, 67037 Strasbourg Cedex 02, France*
[b] *Laboratoire de Catalyse et Synthèse Organique, Faculté des Sciences, Université de Tlemcen BP119, Algeria*

Received 14 May 2007; received in revised form 17 August 2007; accepted 21 August 2007
Available online 25 August 2007

Abstract

Beta zeolite coated on a preshaped medium surface area silicon carbide (SiC) carrier was prepared via a hydrothermal synthesis. The SiC support allows the precise control of the macroscopic shape of the final catalyst, which significantly decreases the diffusion pathway of the reactants to the active site. ^{27}Al MAS-NMR analysis revealed that all the aluminum was in a tetrahedral coordination and no trace of extraframework aluminium was observed. The full width at half maximum of the NMR peak was about 10 ppm, which indicates the presence of small zeolite crystals inside the sample. SEM observation has shown that the zeolite homogeneously coated the outer surface of the silicon carbide extrudate support with different size and shape and random orientation. The existence of a layer of silica and silicon oxycarbide on the surface of the support allows a strong anchoring of the coated zeolite which prevents the loss of the deposited zeolite during handling and operation. The as-prepared catalyst exhibits a high catalytic activity in the benzoylation of anisole in a fixed-bed configuration. In addition, the catalyst was extremely stable, as no deactivation was observed after several hours of test, whereas bulk zeolite exhibits a strong deactivation with the time mainly due to the formation of carbonaceous residues inside the channel network.

Keywords: Friedel-Crafts acylation; Supported BETA zeolite; Silicon carbide

1. Introduction

Zeolite materials are employed in many processes such as supports or sorbents for gas separation. The most promising field is the heterogeneous catalysis, i.e., selective alkane isomerization [1,2], non-oxidative methane aromatization [3,4], cracking [5,6] and Friedel-Crafts reactions [7–14]. The Friedel-Crafts reaction is involved in manufacturing fine and speciality chemicals to produce aromatic ketones, which are important intermediates compounds for pharmaceutical and chemical industries [15,16]. Generally, the most widely used catalysts for this kind of reactions are soluble Lewis acids, i.e., $AlCl_3$, $FeCl_3$ [17], or strong mineral acids such as HF [18]. The major drawbacks are linked with environmental concerns due to the excessive generation of wastes along with corrosion problems, and the impossibility of regeneration. In addition, the formation of complexes between the acid catalysts and the produced ketone leads to a gradual loss of activity and a separation post-reaction is further needed to recover the formed ketone. Recently, the heterogenization of the Friedel-Crafts reactions has received an increasing interest in order to meet the new environmental regulations. This could be achieved by replacing the homogeneous Lewis or mineral acids by heterogeneous catalysts such as zeolites, clays, Nafion-H and heteropoly acids [10–15]. Fixed-bed Friedel-Crafts reactions using zeolites catalysts have been reported by Rhodia for the synthesis of 4-methoxyacetophenone and 3,4-dimethoxyacetophenone [19,20]. However, the intrinsic catalytic activity, especially in a fixed-bed configuration still needs to be improved. Moreover, problems linked to deactivation by dealumination, formation of coke on the acid sites, or by strong product adsorption, have to be solved.

Zeolites are widely synthesized by hydrothermal process with different size depending on the nature of the starting gel and its composition [21]. The as-prepared zeolite in its bulk form is a

* Corresponding author. Tel.: +33 3 90 24 26 75; fax: +33 3 90 24 26 33.
E-mail address: gauthier.wine@ecpm.u-strasbg.fr (G. Winé).
[1] Part of the ELCASS (European Laboratory of Catalysis and Surface Science).

1381-1169/$ – see front matter © 2007 Elsevier B.V. All rights reserved.
doi:10.1016/j.molcata.2007.08.018

highly dispersed powder and consequently, recovery at the end of the synthesis by centrifugation and filtration is often difficult. Such problems are more pronounced in the case of beta zeolite nanocrystals with sizes as small as 10 nm which requires an ultra-centrifugation technique for separation.

Finally, it should be noted that macroscopic shape zeolites generally receive an additional shaping step by mixing with binders before extrusion. By this method, part of the zeolite is covered by the binder and thus, is not accessible for the reactants. The presence of the binder also increases diffusion problems and reduces the accessibility to the porosity of the zeolite phase. It is thus of interest to find new synthesis methods in order to reduce the synthesis duration and to avoid the binder addition for the final shaped zeolite materials by preparing zeolite with direct controlled macroshape. Several groups have reported the synthesis of supported zeolite on different supports and matrix materials such as alumina, silica, ceramic monolith and carbon [22–27].

Silicon carbide exhibits a high thermal conductivity, a high resistance towards oxidation, a high mechanical strength and chemical inertness, which are properties required for heterogeneous catalyst support materials. All of these advantages lead to the conclusion that silicon carbide is a promising candidate for use as heterogeneous catalyst support in place of the classical supports such as alumina or silica, especially in reactions with high thermal transfers, and in harsh environment media. It has been shown that silicon carbide could be efficiently used as support for zeolite composites [14,28,29], thanks to its physicochemical properties. No support dissolution during the zeolite synthesis in a very basic medium was observed: this could modify the molar ratio of the gel solution, and as a consequence the acidic nature of the zeolite itself. Then, such composites could be used either as catalyst support or as catalyst in an aggressive media without problems linked to the corrosion. The high oxidation resistance of the silicon carbide is compatible with oxidative atmosphere.

The aim of the present article is to report the synthesis of supported BEA on macroscopic SiC in extrudates form. The as-synthesized material was subsequently tested as catalyst in a Friedel-Crafts reaction in a fixed-bed configuration. The observed Friedel-Crafts activity on the BEA/SiC catalyst was compared with the one of the bulk zeolite. The catalyst, before and after reaction, was characterized by several techniques in order to get more insight on the nature of the active phase and to understand the differences in terms of deactivation.

2. Experimental

2.1. Support

Silicon carbide in an extrudate form (diameter, 2 mm, length, 6 mm) with a specific surface area of 23 $m^2\ g^{-1}$ and a mesopores size centered at around 40 nm, measured both by N_2 adsorption and by mercury intrusion, was used as support for subsequent zeolite synthesis. The later method also reveals the presence of a large amount of macropores centered at about 0.07 μm (Fig. 1). The support was synthesized according to a gas–solid

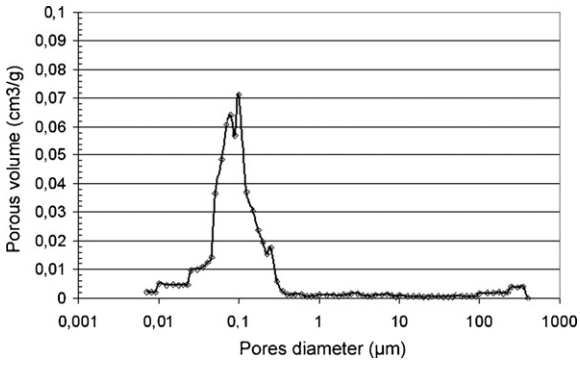

Fig. 1. Mercury intrusion of SiC.

reaction between SiO and carbon according to the Shape Memory Synthesis method [30]. Due to the synthesis method using an intimate gas–solid reaction between the SiO and solid carbon with a concomitant release of gaseous CO, no microporosity was generated inside the solid. XPS analysis has shown that the SiC surface was constituted by about 40 at.% of SiC, 30 at.% of SiO_2 and 30 at.% of SiO_xC_y [30]. The SiO_2 and SiO_xC_y phases were expected to be formed during the synthesis owing to the presence of a small amount of oxygen in the flushing Ar flow (10 ppm) and also during the handling of the sample in air. These oxidic phases are probably formed on the highly reactive defect sites of the sample. Before the synthesis, the SiC material was calcinated in air at 900 °C for 2 h in order to transform the SiO_xC_y topmost layer into the corresponding SiO_2. The specific surface area of the calcined sample measured by the BET method was 20 $m^2\ g^{-1}$, while almost no porosity change has been observed. It should also be noted that the SiC exhibits a relatively high proportion of macropores, which represent about 33% of the total pore volume according to the mercury penetration measurement.

2.2. Supported HBEA synthesis

The supported zeolite synthesis was carried out in a hydrothermal mode using the following precursor solution composition: SiO_2:Al_2O_3:TEAOH:H_2O (50:1:14:370) [31]. The SiC extrudates (10 g) were then added to the gel solution, followed by 1 h aging at room temperature. The mixture was then transferred into an autoclave lined with PTFE and the synthesis was carried out during 48 h under hydrothermal conditions at 140 °C. After synthesis, the composite extrudates were rinsed several times with distilled water and filtered. Then the solid was sonicated in an ethanol solution during 10 min in order to remove the remaining gel or weakly adsorbed zeolite particles. The resulting wet solid was subsequently dried in air at 100 °C during one night. The organic structurant was removed by heating the sample in flowing argon at 550 °C for 14 h. The as-prepared BETA zeolite/SiC was exchanged overnight with NH_4–Cl aq (1 M, 150 ml) at 90 °C to obtain the NH_4-form. The H-BETA form was obtained by calcination of the sample in air at 550 °C for 10 h. The obtained HBEA has a Si/Al ratio of 25.

For comparison, a commercial HBEA zeolite (Zeolyst International, Si:Al ratio of 12.5) was also tested in the same reaction conditions. The commercial HBEA was obtained by calcinating

the NH_4-BEA in air at 550 °C for 10 h. The powder was then pasted, crushed and sieved in order to obtain a granulometry between 0.4 and 1 mm.

2.3. Characterization techniques

Structural characterization of the samples was done by XRD measurements carried out with a Siemens D-5000 powder X-ray diffractometer ($\theta/2\theta$), using Cu Kα radiation, with long time scan (10 s) and small step scan (0.02°). The nature of the different phases present in the sample was checked using the database of the Joint Committee on Powder Diffraction Standards (JCPDS). The average particle size was deduced from the X-ray line broadening using the Scherrer equation.

The morphology of the sample was investigated using a Scanning Electron Microscopy (SEM) Jeol XL 30 FEG microscope.

The pore size and the surface area measurements were performed on a Coulter SA-3100 porosimeter using nitrogen as adsorbat at liquid nitrogen temperature. Before each measurement, the sample was evacuated at 300 °C for 14 h in order to desorb impurities adsorbed on the surface.

^{27}Al ($I = 5/2$) magic angle spinning nuclear magnetic resonance (MAS-NMR) was carried out with a Brucker DSX 400 spectrometer operating at $B_0 = 9.4$ T (Larmor frequency $\nu_0 = 104.2$ MHz). A single pulse of 0.8 ms with a recycle delay of 1 s was used for all experiments. The spinning frequency was 8 kHz. Measurements were carried out at room temperature with $[Al(H_2O)_6]^{3+}$ as external standard reference.

The temperature-programmed oxidation (TPO) were carried out on a 200 mg sample, under a flow of O_2 (10% in He) at 50 cm^3 min^{-1}, from room temperature to 800 °C at 10 °C min^{-1}. A Saturn 3 Varian mass spectrometer was used to analyze the outlet gas-phase composition and to follow the signal of CO ($m/e = 28$) and CO_2 ($m/e = 44$). Calibration was realized using known amounts of Mo_2C. For each sample, the results were normalized versus the amount of zeolite.

2.4. Fixed-bed Friedel-Crafts reaction

The catalytic test was carried out in a tubular glass reactor (10 mm inner diameter and 200 mm length) in a trickled-bed mode at a reaction temperature of 120 °C with a supported catalyst weight of 2 g (0.2 g in the case of pure HBEA) supported on a fritted disk. The top of the catalyst was filled with a quartz wool plug in order to avoid the formation of preferential channels through the catalyst bed. The catalytic activity, expressed in terms of conversion, was calculated based on the benzoyl chloride per gram of zeolite in the reactor. The liquid reactants, composed by a mixture of anisole and benzoyl chloride (Fig. 2) with a molar ratio of 8, was injected on the top of the reactor by a HPLC pump (Varian 9020 HPLC) with different liquid rates ranging from 0.1 to 0.5 ml min^{-1} corresponding to a Weight Hour Space Velocity (WHSV) from 4 to 20 h^{-1}. The liquid exiting exits the reactor was withdrawn at regular time intervals and the products distribution was analyzed using Gas Chromatography (GC, Varian 3400) equipped with a PONA column. The catalytic performance was compared with that of the commercial unsupported zeolite under similar reaction conditions. Before the test, the commercial zeolite in powder form was pressed, crushed, and sieved, and the fraction between 0.4 and 1 mm was retained for the test.

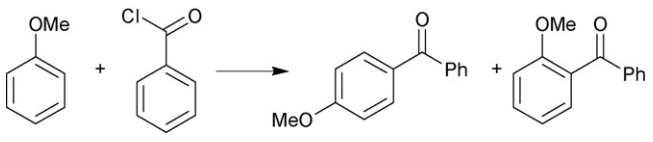

Fig. 2. Benzoylation of anisol by benzoyl chloride.

3. Results and discussion

3.1. HBEA/SiC characteristics

The first advantage of the supported zeolite was the complete avoidance of post-synthesis centrifugation of the crystallized nano-zeolite which is a time and energy consuming process. In the present case, the product was simply filtered over a fritted disk and washed before calcination in flowing argon at 550 °C in order to remove the remaining organic template. The loading of the zeolite on the SiC can be calculated by measuring the weight loss after HF dissolution of the composite BETA/SiC: it was estimated at 10 wt.% according to the synthesis conditions.

The XRD pattern of the as-synthesized catalyst after calcination and ammonium exchange is presented in Fig. 3. The two characteristic diffraction lines corresponding to the BETA zeolite phase (space group $P4_122$) were clearly observed along with those of the SiC support. No trace of other compounds, such as alumina or silica, has been observed, which indicates the high purity of the obtained zeolite. It is significant to note that the diffraction lines corresponding to the BETA zeolite were already visible in the pattern after only about 12 h of synthesis. On the other hand, Tosheva et al. [27] have reported that the crystallization rate of BETA zeolite was slightly lowered when the support was introduced into the mother liquor due to the existence of diffusional phenomenon, even at higher synthesis temperature, i.e., 170 °C. Apparently, the SiC support provides a more beneficial effect on the crystallization behavior of the zeolite. The SiC support, after pre-calcination in air at 900 °C, probably contains a high density of defects on its surface, which allows a rapid

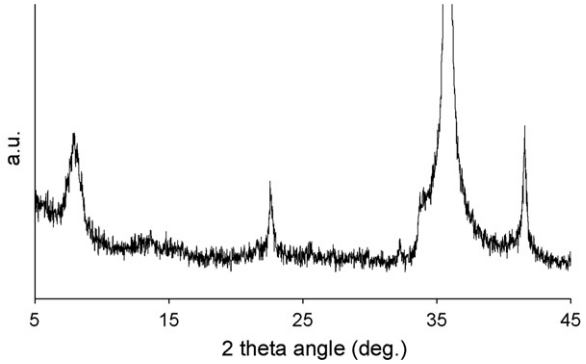

Fig. 3. XRD Pattern of the H-BEA/SiC.

nucleation at the beginning of the synthesis which thus increasing the yield of the synthesis. The presence of a high amount of macropores inside the SiC allows the easy filling of the support with the starting gel, without the pore entrance plugging as in the case of small pores, leading to an homogeneous layer of zeolite inside the support matrix. The high chemical inertness of the ceramic support towards corrosion allows to reduce the modification of the reactants different concentrations inside the solution which could also improve the crystallization rate.

The zeolite formation was also confirmed by ^{27}Al MAS-NMR (Fig. 4). The aluminum NMR peak was visible at 50 ± 2 ppm and could be unambiguously attributed to the tetrahedral coordinated aluminum atoms in the zeolite framework, in agreement with earlier ^{27}Al MAS-NMR studies of zeolite samples in the literature [24]. The absence of ^{27}Al resonance at around 0 ppm indicates that no trace of octahedral aluminium, resulting from the precipitation of aluminium outside the zeolite framework, nor distorted tetrahedral aluminum species [24] have been formed during the synthesis. Such a result indicates that all the aluminium atoms were incorporated into the TO_4 (T standing for Si or Al) framework of BEA and that no bulk alumina was formed, in good agreement with the XRD observations. The FWHM of the ^{27}Al peak was around 12 ppm. This value reflects a relatively small crystal size of the as-prepared zeolite according to van Grieken et al. [32] and Jacobsen et al. [24]. Jacobsen et al. [24] have reported a FWHM of 7.1 ppm for large ZSM-5 crystals (8 μm) whereas for small size ZSM-5 crystals (nanometer size) the FWHM significantly increased to about 10.6–11.1 ppm. The average zeolite particle size determined by the NMR results is in good agreement with that observed by XRD and SEM (see below).

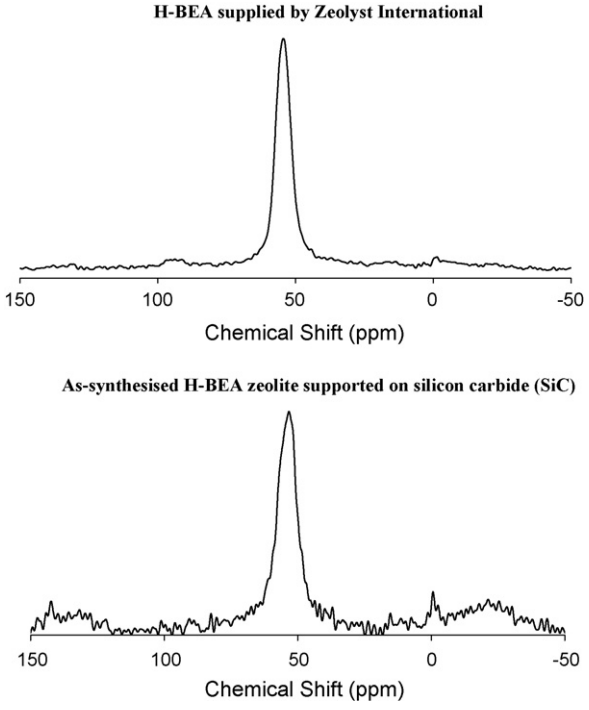

Fig. 4. ^{27}Al MAS-NMR spectrum of the H-BEA/SiC and the bulk commercial H-BEA samples.

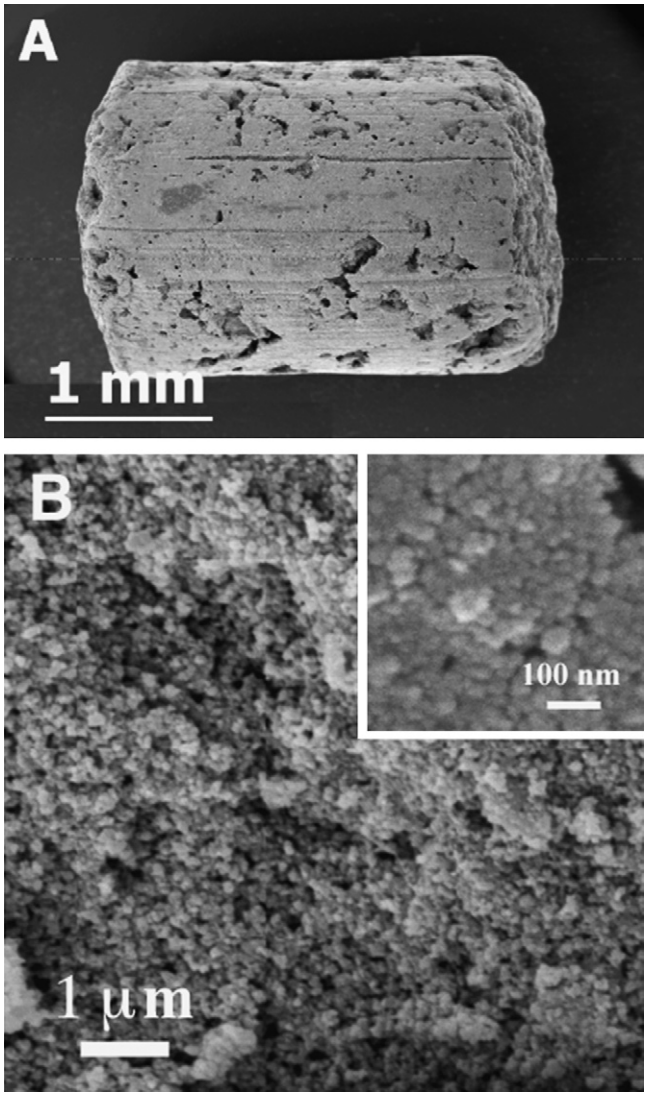

Fig. 5. SEM images of the H-BEA/SiC sample.

The SEM image of the gross morphology of the sample is displayed in Fig. 5A. It shows that the extrudate morphology of the support was not modified during the synthesis. High magnification SEM image (Fig. 5B) reveals the formation of beta zeolite with a homogeneous size, covering the entire surface of the silicon carbide support. The as-synthesized zeolite has an average particle size of around 30 nm as shown by the SEM image in the inset of Fig. 5B. The zeolite particles were randomly distributed over the support surface with a high voids fraction. It should be noted that the zeolite layer formed in the present work consisted in several aggregates of zeolite particles and not in a continuous film as reported by Gavalas and co-workers [13] and by van der Puil et al. [23] for instance. This could be attributed to differences between the nutrient solutions used in the present work and those used by van der Puil [23] and by Gavalas and co-workers [13], or also between the synthesis conditions. The difference between the SiO_2/SiC surface and the low surface area alumina [13] could also play a role. According to the SEM images, zeolite particles were homogeneously dispersed throughout the porosity of the SiC support,

considering taking into account the relatively high viscosity of the synthesis gel employed in the present work. The high penetration of zeolite particles inside the support was attributed to its high macroporosity which favors the gel penetration during the filling process. It should also be noted that the zeolite particle size inside the support porous network was almost similar to that observed on the outer surface. This indicates that the rate of nucleation was similar, which is in line with the ease of diffusion of the synthesis gel into the support.

The mechanical anchorage of the zeolite on the SiC support surface was evaluated by submitting the sample to sonication treatment for 1 h. The total weight loss after such a treatment was about 2 wt.% of the deposited zeolite, which indicates that the zeolite material was strongly bonded to the support surface. It was not the case over other supports such as alumina or silica. Indeed removal of a significant amount of zeolite crystallites by sonication has been reported by van der Puil et al. [23] on alumina extrudates and was attributed by the authors to the weak interaction and bonding between the zeolite crystallites and the support surface. Beers et al. [7] have reported that the anchorage strength can be significantly improved using silica binder. In our case, the silica layer formed on the outer surface of the SiC support probably induces the formation of a strong interface between the support and the deposited zeolite, which prevents its mechanical loss during the sonication treatment. The presence of such a layer probably allowed the good wetting of the zeolite coating. During the hydrothermal synthesis, it was expected that the chemical interaction between the support and the gel phase, both containing silicon entities, and the proper characteristics of each phase, constituted important parameters in order to obtain a homogeneous and stable zeolite coating layer. It was proposed that the zeolite was chemically bonded to a layer of SiO_2 which was directly generated by air oxidation of the SiC sample. SiC supported zeolite can be synthesized directly by contacting the SiC support with a layer of SiO_2 to a solution containing aluminum source [33]. The as-synthesis material exhibits an extremely high mechanical anchorage which confirms the hypothesis concerning the mode of formation of the zeolite on the topmost layer of the SiC support through partial dissolution-recrystallization of the thin SiO_2 layer covering the SiC surface. This is not expected to occur on an alumina surface because of the absence of Si atoms in the support and results in the zeolite loss during the sonication treatment. Van der Puil et al. [20] have indeed reported that pretreatment of the starting alumina by a template solution containing Si, resulted in an improvement of the interaction between the support and the gel medium.

The formation of zeolite on the surface of the SiC support also significantly increases the overall specific surface area of the composite from 25 to about 120 $m^2\,g^{-1}$. The contribution of the microporous porosity is 60 $m^2\,g^{-1}$. Considering the weight of the deposited zeolite and the hypothesis that the SiC surface remains unmodified after the synthesis, the intrinsic specific surface area of the as-synthesized zeolite was calculated to be around 500 $m^2\,g^{-1}$. S_{BET} of the commercial sample is 680 $m^2\,g^{-1}$. The increase of the specific surface area and the formation of micropores were directly attributed to the presence of zeolite crystallites with high specific surface area amounting to several hundred square meters according to literature results [31,34].

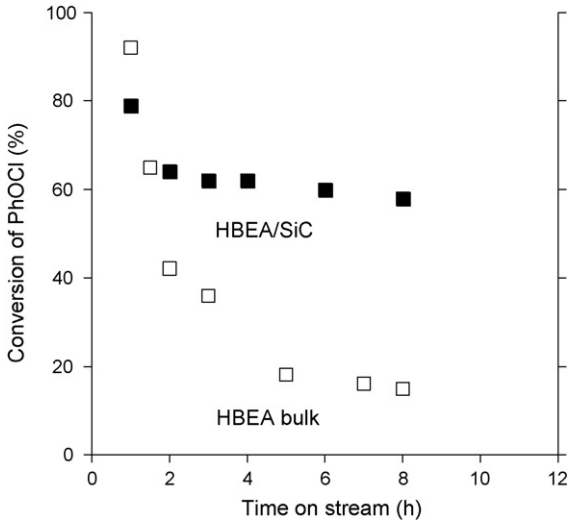

Fig. 6. Benzoylation activity over H-BEA/SiC and commercial H-BEA catalysts.

3.2. Fixed-bed Friedel-Crafts reaction

The catalytic results obtained in the Friedel-Crafts reaction over silicon carbide supported HBEA catalyst at a WHSV of 4 h^{-1} are displayed in Fig. 6 as a function of time on stream at 120 °C. As soon as the reactants mixture was in contact with the catalyst, the colorless solution became red, indicating the formation of aromatic ketone on the catalyst surface. The initial benzoylation activity was relatively high after 1 h on stream, i.e., 73% of conversion, with a selectivity towards *para*-methoxybenzophenone of about 96%. Such results are in line with those already reported in the literature for slurry reactor configurations over zeolite catalysts, where the main product is the *p*-substituted ketone [35]. The other reaction products, i.e., *o*-methoxybenzophenone and ester were formed in almost equal concentrations and represent less than 4% of the total reaction products. Previous works concerning the benzoylation of anisole on SBA-15 based material have shown the possibility to produce the phenyl benzoate by esterification of the phenol obtained from the hydrolysis of the anisole [36]. The benzoylation activity slightly decreased from 73 to about 60% after 3 h on stream but remained unchanged up to more than 12 h of test which means that almost no deactivation occurred after 3 h on stream. The selectivity towards *p*-methoxybenzophenone remained unchanged during the whole test which indicates that the nature of the active phase was not modified.

A comparison was also made using unsupported commercial BETA zeolite (Zeolyst International) while keeping the reaction conditions similar. The results obtained are displayed in the same figure. The initial benzoylation activity of the unsupported zeolite was similar to that observed with the supported catalyst, i.e., 70%. However, on the bulk zeolite, the benzoylation activity drastically decreased with time on stream from 70 to about 30% after 6 h of test. This indicates a strong inhibition of the active

sites in the unsupported zeolite during the reaction carried out in a fixed-bed configuration. In this case, the selectivity towards *p*-methoxybenzophenone was also unchanged which indicates that the deactivation was solely due to the active sites loss.

The difference of activity observed between the supported and unsupported HBEA catalysts can be attributed to the average size of the zeolite. On the supported catalyst, the average size of the active zeolite was expected to be smaller than in the case of the unsupported one. The smaller particle size of the supported zeolite was attributed to the presence of the SiC support which prevents excessive aggregation. The bulk zeolite presents large aggregates of small crystals in contrast with the supported catalysts. It presents micrometrics aggregations of small crystals (20 nm) in contrast with the supported catalysts. Such differences significantly influence the rate of reactants and products diffusion thus modifying the stability of the catalyst as a function of time on stream. It has been reported by several authors that the aromatic ketone is a main inhibitor of the Friedel-Crafts reaction in a slurry reactor due to its strong adsorption on the active sites. Derouane and co-workers [8,9] have reported that the acylation activity significantly decreased when increasing the amount of aromatic ketone in the reactants mixture. Similar deactivation has also been reported by Jaimol et al. [37] in a fixed-bed reactor during the acetylation of toluene over H-ZSM5 catalyst. At 453 K, the conversion decreased from 70 to 30% after about 7 h on stream. The deactivation observed was attributed by the authors to coke formation through acidic assisted condensation inside the zeolite microporosity. Freese et al. [38] have reported that the acylation activity on the dealuminated H-BETA was higher than that observed on the initial H-BETA. Such observation was attributed to the porosity modification in the dealuminated H-BETA which favors the diffusion of the products from the core of the catalyst to the surface for desorption, thus preventing excessive coke formation. This coke formation inhibits the access of the reactants to the active phase. According to the observed results, it seems that a balance should be found between the intrinsic activity and acidity strength of the zeolite, the deactivation rate and the pore size, which control the diffusion rate of the reactants and the products in and out of the zeolite porosity network. It is expected that the dispersion of the zeolite particles on the SiC support surface favors the evacuation of the produced ketone when compared to the unsupported zeolite. The higher diffusion rate of ketone out of the supported zeolite porosity probably allows maintaining the initial activity of the supported catalyst despite some slight deactivation. The initial deactivation could be due to the equilibrium adsorption of a part of the formed ketone. The zeolite apparent particle size influences the rate of diffusion of the reactants and products, thus modifying the stability of the catalyst as a function of time on stream. It also and probably increases the coke formation, as a result of a long apparent sejourn time of the products inside the zeolite porosity. Such diffusion phenomenon was expected to be more drastic in a fixed-bed configuration compared with a batch reactor, because the reactants are continuously tickled through the catalyst bed with time on stream, which significantly modify the rate of ketone diffusion out of the zeolite pore and in turn, the rate of reactants diffusing from the outer surface to the zeolite porosity. According to our previous works already published [14,28,29,33], we can assume that the higher activity of the supported zeolite was directly linked to its thin layer with lower diffusional resistance and also to its smaller primary particle size. The same result (not shown) obtained in the direct dehydration of methanol on the supported zeolite, i.e., ZSM-5/SiC [39], also support such assumption.

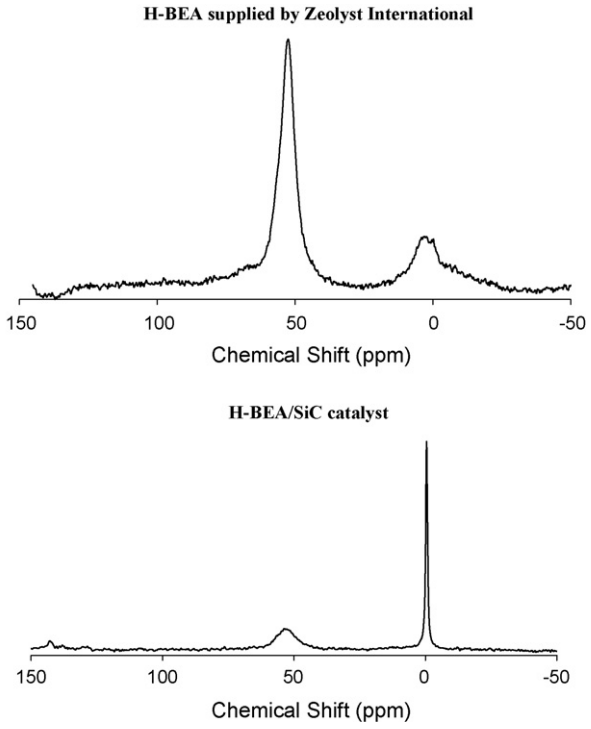

Fig. 7. ^{27}Al MAS-NMR spectra of the spent catalysts.

^{27}Al MAS-NMR was used to characterize the nature of the catalyst after reaction and the results are displayed in Fig. 7. On the unsupported zeolite, a dealumination phenomenon has occurred during the catalytic test, as shown by the appearance of a relatively high resonance peak with similar FWHM located at 0 ppm, i.e., extraframework aluminum. The dealumination phenomenon has already been reported by different authors in the literature for other zeolites [37]. The long stay time of the reaction products, especially HCl, inside the bulk zeolite was expected to be responsible for such dealumination, which contributes to the loss of the acylation activity.

On the supported zeolite, a resonance peak located at 0 ppm was also observed (Fig. 6B). However, the FWHM and the peak profile were completely different compared to that observed on the unsupported H-BEA. It is expected that the resonance peak located at 0 ppm on the supported zeolite was not due to extraframework aluminium, but rather to aluminum species bonded with organic species which remained on the catalyst surface. The absence of deactivation observed on the catalyst also supported this hypothesis [40]. Detailed investigation by ^{27}Al MAS-NMR will be carried out in order to get more insight into the origin of the resonance peak at 0 ppm.

Temperature-programmed oxidation (TPO) was also employed to characterize the amount of carbonaceous species

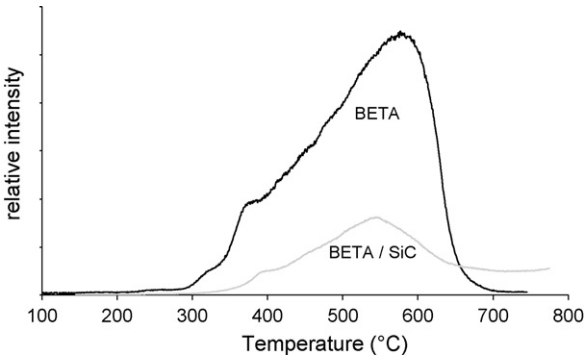

Fig. 8. TPO spectra of the spent catalysts.

formed during the test. The TPO spectra are displayed in Fig. 8. The amount of coke formed on the supported zeolite was lower compared to that obtained on the bulk zeolite, which partly confirms the hypothesis advanced above concerning the rapid diffusion out of the products out of the supported zeolite cavities. The coke formed inside the bulk zeolite was also more graphitized, as shown by the higher oxidation temperature, compared to the one observed on the supported zeolite. This was attributed to be due to the long residence time inside the porosity.

3.2.1. Influence of WHSV

The evolution of the benzoyl chloride conversion versus the time on stream, for three different space velocity (WHSV) values is presented on Fig. 9. At the highest velocity of 500 μl min^{-1}, which corresponds to a WHSV of 20 h^{-1}, the catalytic activity is very low: the conversion is only 25% at the beginning of the test and decreases regularly to 13% after 8 h of time on stream. The activity drop when increasing the reactants velocity was attributed to the fact that at high velocity part of the reactants did not had enough time to reach the active sites inside the zeolite porosity network and thus, was directly escaped from the catalytic bed without reaction. Moreover, the major part of reactants passed through the catalyst without meeting any active site.

Concerning the lower space velocities, i.e., 4 and 10 h^{-1} corresponding, respectively, to 100 and 250 μl min^{-1}, the catalytic

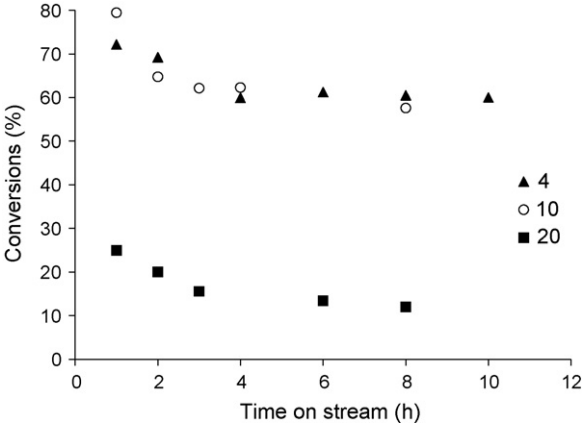

Fig. 9. Benzoylation test over H-BEA/SiC catalyst: influence of WHSV.

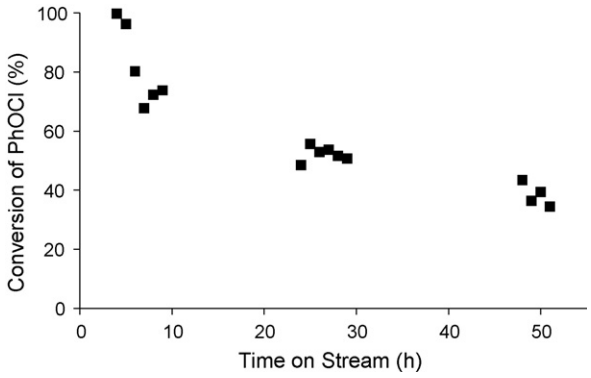

Fig. 10. Long-term benzoylation test over H-BEA/SiC catalyst.

activity are more or less the same: from 80% of conversion at the beginning to 60% at the end. It seems that the BETA/SiC catalyst has a number of active sites which can convert the reactants until an upper limit of velocity.

In all cases, the selectivity towards the *p*-methoxybenzophenone remains higher than 90%.

In view of these results, it can be assumed that the optimal space velocity in these reactions conditions is 10 h^{-1} (250 μl min^{-1}). At this value, the amount of reactants converted versus the time on stream higher than at 4 h^{-1}, without any drop of conversion after 8 h, like at 20 h^{-1}, and with a stable selectivity.

3.2.2. Long-term test

In the present study, the stability of the SiC supported zeolite as a function of the test duration was investigated under the following reaction conditions: catalyst weight, 2 g; zeolite weight, 0.18 g; anisole and benzoyl chloride with a molar ratio of 8; reaction temperature, 120 °C; WHSV, 4 h^{-1}. The results, expressed in terms of conversion and selectivity towards *p*-methoxybenzophenone, are reported in Fig. 10. According to the results some slow deactivation has occurred on the catalyst which could be attributed to the loss of the active site access as a function of time on stream by porosity plugging (Fig. 11) with

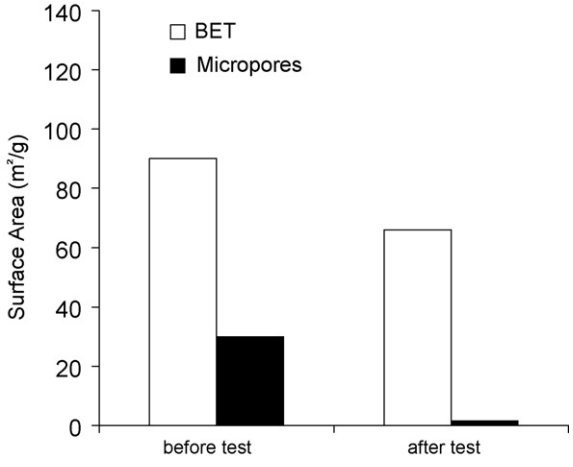

Fig. 11. Porosity distribution of the H-BEA/SiC catalyst before and after benzoylation test.

heavier products. NMR characterization (not shown) did not reveal any dealumination process during the course of the reaction. However, the benzoylation activity after more than 48 h of test still remains gigh (around 35%). On the other hand, the selectivity towards *p*-methoxybenzophenone remained unchanged during the whole test, which highlighting the complete conservation of the active phase.

4. Conclusion

Silicon carbide synthesized by a gas–solid reaction can be efficiently used as support for the synthesis of supported beta zeolite. The high affinity between the SiC surface and the gel precursor led to the formation of a homogeneous layer of zeolite with a high mechanical anchorage. The possibility to prepare SiC with different controlled macroscopic shapes, i.e., extrudates or monolith, allows the abstention of different zeolite supported composites depending on the desired use. The supported BETA zeolite catalyst was active for the benzoylation of anisole by benzoyl chloride and was extremely stable in a fixed-bed reactor configuration. This stability was attributed to the high dispersion of the zeolite layer and the small primary particles size which allow to maintain an equilibrium between the diffusions of the reactants and the products in and out the intraporosity of the zeolite phase. The thin layer of zeolite allows the increase of the product escaping rate and thus, significantly reduce the secondary acidic condensation reactions which could led to the carbonaceous species formation inside the material porosity network compared to that observed on the bulk zeolite. Indeed, in this later, the high length due to the formation of aggregates could increase the sejourn time of the product which could favorize the secondary reactions yielding carbonaceous species. These carbonaceous species were also less graphitized due to the short residence time within the zeolite porosity. However, some deactivation was observed on the supported zeolite for long-term test, which was attributed to a pore plugging. Work is on progress to modify the intrinsic properties of the SiC support, in order to improve the dispersion of the deposited zeolite, and thus significantly improve the catalysts stability.

Acknowledgements

The authors would like to thank Sicat SA (France) for supplying the SiC support, and Severinne Rigolet from the LMM (Mulhouse, France) for the MAS-NMR analysis.

References

[1] J.P. Marques, I. Gener, J.M. Lopes, F. Ramôa Ribeiro, M. Guisnet, Catal. Today 107–108 (2005) 726.
[2] T. Wakayama, H. Matsuhashi, J. Mol. Catal. A: Chem. 239 (2005) 32–40.
[3] H. Liu, X. Bao, Y. Xu, J. Catal. 239 (2006) 441.
[4] V.T.T. Ha, V.T. Le, P. Meriaudeau, C. Naccache, J. Mol. Catal. A: Chem. 181 (2002) 283.
[5] R. Castañeda, A. Corma, V. Fornés, J. Martínez-Triguero, S. Valencia, J. Catal. 238 (2006) 79.
[6] T. Blasco, A. Corma, J. Martínez-Triguero, J. Catal. 237 (2006) 267.
[7] A.E.W. Beers, T.A. Njihuis, F. Kapteijn, J.A. Moulijn, Micro. Meso. Mater. 48 (2001) 279.
[8] E.G. Derouane, G. Crehan, C.J. Dillon, D. Bethell, H. He, S.B. Derouane-Abd Hamid, J. Catal. 194 (2000) 410.
[9] E.G. Derouane, C.J. Dillon, D. Bethell, S.B. Derouane-Abd Hamid, J. Catal. 187 (1999) 209.
[10] R.M. Barrer, Hydrothermal Chemistry of Zeolites, Academic Press, London, 1987.
[11] A.E.W. Beers, T.A. Nijhuis, N. Aalders, F. Kapteijn, J.A. Moulijn, Appl. Catal. 243 (2003) 237.
[12] K. Gaare, D. Akporiaye, J. Mol. Catal. A: Chem. 106 (1996) 177.
[13] R. Lai, Y. Yan, G.R. Gavalas, Micro. Meso. Mater. 37 (2000) 9.
[14] S. Basso, J.P. Tessonnier, G. Winé, C. Pham-Huu, M.J. Ledoux, US Patent Application 20,030,162,649, assigned to Sicat, 2003.
[15] R.A. Sheldon, Chem. Ind. (London) 7 (1992) 903.
[16] T.K. Wan, M.E. Davis, J. Catal. 152 (1994) 25.
[17] G.A. Olah, S. Kobayashi, J. Nishimura, J. Am. Chem. Soc. 95 (1973) 564.
[18] G.A. Olah, Friedel-Crafts and Related Reaction, vol. I–IV, Wiley-Interscience, NewYork/London, 1963–1964.
[19] M. Spagnol, L. Gilbert, E. Benazzi, C. Marcilly, US Patent no. 6,013,840, assigned to Rhodia Chimie, 2000.
[20] M. Spagnol, L. Gilbert, H. Guillot, P. J. Tirel, US Patent no. 6,194,616, assigned to Rhodia Chimie, 2001.
[21] K. Beschmann, L. Riekert, J. Catal. 141 (1993) 548.
[22] G.B.F. Seijger, O.L. Oudshoorn, W.E.J. van Kooten, J.C. Jansen, H. van Bekkum, C.M. van den Bleek, H.P.A. Calis, Micro. Meso. Mater. 30 (2000) 195.
[23] N. van der Puil, F.M. Dautsenberg, H. van Bekkum, J.C. Jansen, Micro. Meso. Mater. 27 (1999) 95.
[24] C.J.H. Jacobsen, C. Madsen, T.V.W. Janssens, H.J. Jakobsen, J. Skibsted, Micro. Meso. Mater. 39 (2000) 393.
[25] J.C. Jansen, J.H. Koegler, H. van Bekkum, H.P.A. Calis, C.M. van den Bleek, F. Kapteijin, J.A. Moulijn, E.R. Geus, N. van der Puil, Micro. Meso. Mater. 21 (1998) 213.
[26] I. Schmidt, A. Boisen, E. Gustavsson, K. Stahl, S. Pehrson, S. Dahl, A. Carlsson, C.J.H. Jacobsen, Chem. Mater. 13 (2001) 4416.
[27] L. Tosheva, B. Mihaolova, V. Valtchev, J. Sterte, Micro. Meso. Mater. 48 (2001) 31.
[28] G. Winé, J.P. Tessonnier, C. Pham-Huu, M.J. Ledoux, Chem. Commun. (2002) 2418.
[29] G. Winé, J. Matta, J.P. Tessonnier, C. Pham-Huu, M.J. Ledoux, Chem. Commun. (2003) 530.
[30] M.J. Ledoux, C. Pham-Huu, CaTTech 5 (2001).
[31] M.A. Camblor, A. Corma, S. Valencia, Micro. Meso. Mater. 25 (1998) 59.
[32] R. van Grieken, J.L. Sotelo, J.M. Menendez, J.A. Melero, Micro. Meso. Mater. 39 (2000) 135.
[33] G. Winé, M.-J. Ledoux, C. Pham-Huu, Top. Catal., in press.
[34] C. Baerlocher, W.M. Meier, D.H. Olsen, Structure Commission of the Internationnal Zeolite Association, fifth ed., Elsevier, 2001.
[35] M. Cidambaram, C. Venkatesan, P. Moraud, A. Finels, A.V. Ramaswany, A.P. Singh, Appl. Catal. 224 (2002) 129.
[36] Z. El Berrichi, L. Cherif, O. Orsen, J. Fraissard, J.P. Tessonnier, E. Vanhaecke, B. Louis, M.J. Ledoux, C. Pham-Huu, Appl. Catal. A 298 (2006) 194.
[37] T. Jaimol, A.K. Pandey, A.P. Singh, J. Mol. Catal. A: Chem. 170 (2001) 117.
[38] U. Freese, F. Heinrich, F. Roessner, Catal. Today 49 (1999) 237.
[39] E. Vanhaecke, S. Ivanova, C. Pham-Huu, C Pham, French Patent, Sicat, in press.
[40] G. Winé, J.P. Tessonnier, J. Matta, S. Rigolet, C. Maréchal, J. Matta, C. Pham-Huu, M.J. Ledoux, Anais do 12° Congresso Brasileiro de Catalise (2003) 132.